AIMS Mathematics, 9(7): 18211–18235.
DOI: 10.3934/math.2024889
Received: 27 March 2024
Revised: 23 May 2024
Accepted: 27 May 2024
Published: 29 May 2024

https://www.aimspress.com/journal/Math

Research article

Threshold analysis of an algae-zooplankton model incorporating general interaction rates and nonlinear independent stochastic components

Yassine Sabbar[1,*] **and Aeshah A. Raezah**[2]

[1] MAIS Laboratory, MAMCS Group, FST Errachidia, Moulay Ismail University of Meknes, P.O. Box 509, Errachidia 52000, Morocco

[2] Department of Mathematics, Faculty of Science King Khalid, University Abha, 62529, Saudi Arabia

* **Correspondence:** Email: y.sabbar@umi.ac.ma; Tel: +212 663662995.

Abstract: The stochastic nature of ecological systems is fundamental to their modeling and understanding. In this paper, we introduce a comprehensive algae-zooplankton model that incorporates general interaction rate and second-order independent stochastic components. Our model's perturbation component encompasses both white noise and jump processes, enabling us to account for various sources of variability and capture a wide range of potential fluctuations in the system. By utilizing an auxiliary equation, we establish a global threshold for the stochastic system, distinguishing between scenarios of extinction and ergodicity. This threshold serves as a critical determinant of the system's long-term behavior and sheds light on the delicate balance between population persistence and decline in ecological communities. To elucidate the impact of noise on the dynamics of algae and zooplankton, we present a series of numerical illustrations. Through these simulations, we highlight how noise influences not only the extinction time but also the shape of the stationary distribution. Our findings underscore the significant role of stochasticity in shaping ecological dynamics and emphasize the importance of considering noise effects in ecological modeling and management practices.

Keywords: algae; zooplankton; Lévy noise; Brownian motion; jumps; dynamics
Mathematics Subject Classification: 37A50

1. Introduction and overview

Stochasticity is inherent in ecological systems, manifesting in myriad ways that shape the destiny of their residents. Stochasticity, characterized by its inherent randomness and unpredictability, is a prime example of this variability, playing a pivotal role in ecological dynamics [1]. The occurrence of

stochastic events, such as unpredictable fluctuations in environmental conditions or chance encounters with predators, introduces a layer of uncertainty that can profoundly impact the survival and evolution of species [2]. For example, consider a population that, under deterministic conditions, would persist indefinitely due to stable environmental factors and abundant resources. Despite apparent resilience, the introduction of stochastic events can dramatically alter the population's trajectory. Sudden environmental disturbances, disease outbreaks, or shifts in predator-prey dynamics can swiftly tip the balance, leading to population declines or even extinction [3].

Generally, the effects of stochasticity are not uniform across species or ecosystems. Some species may possess traits or behaviors that buffer them against the impacts of random events, while others may be more susceptible to stochastic shocks [4]. Additionally, the scale and frequency of stochastic events vary spatially and temporally, further complicating their influence on ecological systems [5]. Understanding the interplay between deterministic and stochastic factors is crucial for comprehending the resilience and vulnerability of ecosystems. While deterministic processes provide a framework for understanding general patterns and trends, stochastic events inject the element of chance that can shape the outcomes in unpredictable ways. Therefore, a holistic approach that considers both deterministic and stochastic forces is essential for effectively managing and conserving biodiversity in a dynamic and uncertain world [6].

The addition of random perturbations in the algae-zooplankton model is motivated by the inherent variability and unpredictability present in natural ecosystems [7]. Environmental fluctuations, such as changes in temperature, light, nutrient availability, and water quality, significantly impact the growth and interactions of both algae and zooplankton populations. Incorporating random perturbations helps capture these environmental variabilities. Additionally, immigration and emigration processes, which are stochastic in nature, can influence population sizes through currents and other physical processes. The interactions between algae and zooplankton are complex and influenced by random predation events and changes in prey availability. Stochastic elements account for the noise and uncertainty in real-world data due to measurement errors and sampling inconsistencies. Understanding how populations respond to random disturbances is crucial for assessing their stability and resilience. Therefore, incorporating random perturbations into the model provides a realistic and comprehensive framework for understanding and predicting the dynamics of these populations in fluctuating environments. In ecological modeling, various methods are employed to introduce variability into ecosystems, each serving different purposes and mimicking distinct aspects of natural dynamics. Among the most common techniques are white noise and Lévy jumps, which play crucial roles in capturing different types of variability within ecological systems.

White noise is a stochastic process characterized by random fluctuations with equal intensity across all frequencies. In ecological contexts, white noise is often used to simulate natural disturbances driven by environmental changes [8]. These disturbances can include fluctuations in temperature, precipitation, or resource availability, as well as disturbances caused by human activities such as logging, pollution, or habitat fragmentation [9]. By incorporating white noise into ecological models, researchers can replicate the unpredictability and variability inherent in natural ecosystems, providing insights into how species and communities respond to environmental fluctuations over time [10]. Building on this approach, certain papers have explored the dynamics between algae and zooplankton under white noise perturbations. For instance:

- In [11], the author introduced a novel approach to modeling the dynamics of algae-zooplankton

systems, incorporating stochasticity through the inclusion of random environmental perturbations represented as white noise. His work yielded insights into the conditions for stochastic extinction, persistence, and the establishment of an ergodic stationary distribution within the system.

- In [12], the authors presented a nutrient-algae model enriched with the incorporation of white noise, aiming to capture the stochastic nature of ecological processes. Their study not only provided insights into the necessary conditions for extinction, persistence, and ergodicity within the model but also shed light on the dynamic interplay between nutrient availability and algae abundance in fluctuating environments.
- In [13], the authors investigated the dynamics of a stochastic system involving toxin-producing algae and fish, incorporating harvesting practices. Their study yielded valuable insights into the system's behavior, offering sufficient conditions for both extinction and persistence.
- In [14], the authors explored the dynamics of a stochastic model concerning algae-zooplankton interactions, taking into account variations in algae cell size and zooplankton body size. The authors derived criteria for both extinction and ergodicity within the model.

On the other hand, pure Lévy jumps represent a type of stochastic process characterized by infrequent but intense changes in a system's state [15]. Unlike white noise, which generates random fluctuations of relatively constant magnitude, pure Lévy jumps simulate abrupt and extreme events that can have significant impacts on ecological dynamics. These events may include rare but severe disturbances such as wildfires, hurricanes, or disease outbreaks, as well as sudden shifts in population dynamics due to predator-prey interactions or competitive pressures [16]. By incorporating pure Lévy jumps into ecological models, researchers can explore the effects of these rare but influential events on the resilience and stability of ecosystems, shedding light on how ecosystems respond to and recover from extreme perturbations. Expanding upon this methodology, specific studies have delved into the interplay between algae and zooplankton dynamics, incorporating the concept of Lévy jumps. For example:

- In [17], the authors introduced a stochastic model of nutrient-plankton food chains, incorporating Lévy jumps into their framework. They established necessary conditions for both the persistence and extinction of plankton populations within the model.
- In [18], the authors introduced an ecological system subjected to high-order white noise and quadratic Lévy jumps. They delineated the conditions governing the extinction and ergodic behavior of the model, offering valuable insights into the long-term dynamics and stability of the system under stochastic perturbations.

By integrating both white noise and pure jumps into ecological modeling frameworks, researchers can capture a wide range of variability and complexity in natural systems. This comprehensive approach enables scientists to investigate how different types of disturbances and environmental changes shape the dynamics of ecological communities, helping to inform conservation and management strategies in an ever-changing world. Additionally, understanding the interplay between different sources of variability can provide valuable insights into the adaptive capacity of species and ecosystems, aiding efforts to predict and mitigate the impacts of global environmental change.

In this paper, we present a general ecological model that incorporates two distinct sources of jumps, each tailored to capture specific aspects of stochasticity within natural systems. Firstly, we integrate second-order white noises, meticulously designed to account for the subtle yet impactful

fluctuations that characterize small-scale variations in environmental conditions. These fluctuations, although seemingly minor, can have profound effects on ecosystem dynamics, influencing everything from population dynamics to community structure. Secondly, we introduce second-order pure jumps, strategically employed to capture the abrupt and intense changes that typify heavy perturbations within ecological systems. These jumps represent the sudden shifts and disturbances that can arise from various factors, such as extreme weather events, sudden changes in resource availability, or outbreaks of disease.

Crucially, we introduce a parameter ranging between 0 and 1, offering the flexibility to personalize the perturbation characteristics and providing insight into both subtle and heavy variations. This parameterization allows us to systematically explore the effects of different levels of perturbation intensity on ecosystem dynamics, offering a nuanced understanding of how ecological systems respond to environmental variability across a spectrum of conditions.

A notable feature of our study is the establishment of a global threshold delineating the boundary between extinction and ergodicity within the model. This threshold plays a pivotal role in distinguishing between two critical scenarios: The sustained persistence of ecological communities (ergodicity) and their eventual decline and disappearance (extinction). By identifying and elucidating this threshold, we offer valuable insights into the underlying mechanisms governing the long-term stability and resilience of algae-zooplankton communities.

The remainder of this paper is organized as follows: Section 2 introduces the algae-zooplankton model and its stochastic formulation. Following this, we present some preliminary concepts and lemmas. In Section 3, we unveil the main theorems that establish the global threshold between extinction and ergodicity within the stochastic model. Section 4 provides numerical illustrations to examine the impact of noise on the dynamics of algae and zooplankton. Finally, we conclude with a discussion of our findings and a consideration of our limitations.

2. Stochastic system and preliminaries

Drawing upon the model outlined in [14], we proceed to introduce a refined algae-zooplankton system that builds upon and extends previous findings in the field. Our system encapsulates the intricate interplay between algae y_0 and zooplankton y_1 dynamics, aiming to elucidate the underlying mechanisms governing their interactions within aquatic ecosystems. The model under perturbation is structured as follows:

$$\begin{cases} \mathrm{d}y_0(t) = \left(\dfrac{ry_0(t)}{s_1 r^2 + s_2 r + s_3} \left(1 - \dfrac{y_0(t)}{L}\right) - \dfrac{\beta_0 y_0(t) y_1(t)}{\gamma y_0(t) + y_1(t)} e^{\left\{-\frac{1}{\zeta_1}(r-\zeta_2 u)^2\right\}} \right) \mathrm{d}t + \varpi_{00} y_0(t) \mathrm{d}S_0(t), \\ \mathrm{d}y_1(t) = \left(\dfrac{\alpha\beta_0 y_0(t) y_1(t)}{\gamma y_0(t) + y_1(t)} e^{\left\{-\frac{1}{\zeta_1}(r-\zeta_2 u)^2\right\}} - \beta_1 y_0(t) y_1(t) - d_1 y_1(t) \right) \mathrm{d}t + \varpi_{10} y_1(t) \mathrm{d}S_1(t), \\ y_1(0) \in \mathbb{R}_+, \quad y_1(0) \in \mathbb{R}_+, \end{cases} \tag{2.1}$$

where r is the size of the algae cells, s_1, s_2, and s_3 are some experimental coefficients, L is the significant ecological carrying capacity, β_0 is the peak consumption rate, γ is the saturated coefficient, ζ_1 and ζ_2 are the usage rate coefficients, u is the metric for zooplankton morphology, α is the transition rate of y_1, β_1 is the toxic emission, d_1 is the mortality rate of y_1, and ϖ_{00} and ϖ_{10} represent the intensity of noise for the independent standard Brownian motions $S_0(t)$ and $S_1(t)$, respectively.

In the complex ecosystems of aquatic environments, the predation dynamics between zooplankton and phytoplankton are closely tied to the size disparities among these tiny organisms. A key principle recognized by ecologists is that larger-bodied zooplankton typically prey on smaller-bodied phytoplankton [19–21]. However, as the ecosystem becomes more populated with multiple species of both phytoplankton and zooplankton, each with varying body sizes, the predation dynamics become increasingly intricate. In these multifaceted scenarios, interactions among planktonic organisms are often complicated by mutual interference, resulting in complex webs of predation and resource use. Consequently, the incidence rates that describe these interactions must take on specific forms to accurately reflect the nuanced relationships at play. Understanding these specific forms of incidence rates is crucial for elucidating the detailed mechanisms governing predator-prey interactions and species coexistence within aquatic ecosystems.

In the model described in [14], the authors focused on the nonlinear interaction function $\frac{\beta_0 y_0(t) y_1(t)}{\gamma y_0(t)+y_1(t)}$. However, real-world scenarios and certain modeling requirements may necessitate a more versatile approach. In order to accommodate a broader range of situations, this paper will explore a generalized functional interaction function $f(y_0(t), y_1(t))$. By doing so, we aim to encompass a wider spectrum of epidemiological dynamics and provide a more flexible framework for modeling ecological competition in various contexts. The generalized form of the system (2.1) is presented as follows:

$$\begin{cases} \mathrm{d}y_0(t) = \left(\dfrac{r y_0(t)}{s_1 r^2 + s_2 r + s_3} \left(1 - \dfrac{y_0(t)}{L}\right) - f(y_0(t), y_1(t)) y_1(t) e^{\left\{-\frac{1}{\zeta_1}(r-\zeta_2 u)^2\right\}} \right) \mathrm{d}t + \varpi_{00} y_0(t) \mathrm{d}S_0(t), \\ \mathrm{d}y_1(t) = \left(\alpha f(y_0(t), y_1(t)) y_1(t) e^{\left\{-\frac{1}{\zeta_1}(r-\zeta_2 u)^2\right\}} - \beta_1 y_0(t) y_1(t) - d_1 y_1(t) \right) \mathrm{d}t + \varpi_{10} y_1(t) \mathrm{d}S_1(t), \\ y_0(0) \in \mathbb{R}_+, \quad y_1(0) \in \mathbb{R}_+, \end{cases} \tag{2.2}$$

where $f \in \mathbb{C}^2(\mathbb{R}_+ \times \mathbb{R}_+, \mathbb{R}_+)$ is an uniformly continuous function such that

$$\frac{\partial f(y_0(t), y_1(t))}{\partial y_1(t)} \leq 0 \leq \frac{\partial f(y_0(t), y_1(t))}{\partial y_0(t)} \leq \vartheta,$$

for a given positive constant ϑ. This generalized function, as described under the aforementioned conditions, includes several specific cases outlined in Table 1 (see, for example, [22–26]).

Table 1. List of some examples of the general interference function f.

Name	*Expression*
Bilinear	$f(y_0, y_1) = y_0,$
Saturated	$f(y_0, y_1) = \dfrac{y_0}{m_0 + y_0}, (m_0 > 0)$
Crowley-Martin	$f(y_0, y_1) = \dfrac{y_0}{(m_0 + y_0)(m_1 + y_1)}, (m_0, m_1 > 0)$
Beddington-DeAngelis	$f(y_0, y_1) = \dfrac{y_0}{1 + m_0 y_0 + m_1 y_1}, (m_0, m_1 > 0)$
Modified Crowley-Martin	$f(y_0, y_1) = \dfrac{y_0}{m_0 + m_1 y_0 + m_2 y_1 + m_3 y_0 y_1}, (m_0, m_1, m_2, m_3 > 0)$

Having expanded the incidence rate to a more generalized form, we are now poised to introduce our

novel model, enriched with second-order perturbations [26, 27]. Consider the following system:

$$\begin{cases} \mathrm{d}y_0(t) = \left(\dfrac{ry_0(t)}{s_1r^2 + s_2r + s_3}\left(1 - \dfrac{y_0(t)}{L}\right) - f(y_0(t), y_1(t))y_1(t)e^{\left\{-\frac{1}{\zeta_1}(r-\zeta_2u)^2\right\}}\right)\mathrm{d}t \\ \qquad\quad +p\displaystyle\sum_{i=0}^{1}\varpi_{0i}y_0^{i+1}(t)\mathrm{d}S_0(t) + (1-p)\int_{\mathbb{R}^2\setminus\{0\}}\sum_{j=0}^{1}\nu_{0j}(\xi)y_0^{j+1}(t_-)D_0(\mathrm{d}t, \mathrm{d}\xi), \\ \mathrm{d}y_1(t) = \left(\alpha f(y_0(t), y_1(t))y_1(t)e^{\left\{-\frac{1}{\zeta_1}(r-\zeta_2u)^2\right\}} - \beta_1y_0(t)y_1(t) - d_1y_1(t)\right)\mathrm{d}t \\ \qquad\quad +p\displaystyle\sum_{i=0}^{1}\varpi_{1i}y_1^{i+1}(t)\mathrm{d}S_1(t) + (1-p)\int_{\mathbb{R}^2\setminus\{0\}}\sum_{j=0}^{1}\nu_{1j}(\xi)y_1^{j+1}(t_-)D_1(\mathrm{d}t, \mathrm{d}\xi), \\ y_0(0) \in \mathbb{R}_+, \quad y_1(0) \in \mathbb{R}_+. \end{cases} \tag{2.3}$$

Here, $S_k(t)$ $(k = 0, 1)$ denotes two mutually independent Standard Brownian motions (SBMs) of strengths $\varpi_{0i} > 0$ $(i = 0, 1)$ and $\varpi_{1i} > 0$ $(i = 0, 1)$, respectively. These SBMs are essentially defined on a filtered probability triple (stochastic basis) $(\Omega, \mathcal{F}_\Omega, (\mathcal{F}_{\{\Omega,t\}})_{t\geqslant 0}, \mathbb{P})$ equipped with a filtration satisfying the usual criteria [4]. $y_k(t^-)$ $(k = 0, 1)$ is the left limits of $y_k(t)$ $(k = 0, 1)$. $\bar{D}_k$ $(k = 0, 1)$ are two independent stochastic Poisson processes related to the measures m_k $(k = 0, 1)$ defined on a measurable set $\mathbb{R}^2 \setminus \{0\}$ as follows:

$$m_k(A) = \int_{\mathbb{R}^2\setminus\{0\}}\int_{\mathbb{R}_+}\alpha_s^{-\alpha_s-1}e^{-t}\mathbb{1}_A(tx)\mathrm{d}tR_k(\mathrm{d}x), \quad A \in \mathcal{B}(\mathbb{R}^2 \setminus \{0\}), \tag{2.4}$$

where $\mathbb{1}$ denotes the indicator function, $\alpha_s \in (0, 2)$, and R_k is the Rosiński measure defined on $\mathbb{R}^2 \setminus \{0\}$ such that $R_k(0) = 0$, $(k = 0, 1)$, with $\displaystyle\int_{\mathbb{R}^2\setminus\{0\}}\left(\|x\|^2 \wedge \|x\|^{\alpha_s}\right)R_k(\mathrm{d}x) < \infty$, $\alpha_s \in (0, 2)$ (for more details, please see [28]). D_k $(k = 0, 1)$ are two independent compensated Poisson random measures such that $D_k(\mathrm{d}t, \mathrm{d}\xi) = \bar{D}_k(\mathrm{d}t, \mathrm{d}\xi) - m_k(\mathrm{d}\xi)\mathrm{d}t$. $\nu_k : \mathbb{R}^2 \setminus \{0\} \to \mathbb{R}$ are the jumps size functions which are postulated to be positive and continuous on $\mathbb{R}^2 \setminus \{0\}$, for all $i, k = 0, 1$. It is assumed that $\displaystyle\int_{\mathbb{R}^2\setminus\{0\}}\nu_{ik}^2(\xi)m_i(\mathrm{d}\xi)$ is finite. The variable p is a constant between 0 and 1. This is included in order to have the possibility of personalizing the influence of the noise part (from a modeling perspective). If $p = 1$, system (2.3) simplifies to a model featuring solely second-order white noise, effectively simulating continuous and Gaussian variations commonly observed in ecological systems. Conversely, when $p = 0$, system (2.3) transforms into a model characterized by unexpected jumps with heavy tails, resulting in abrupt and drastic changes in species dynamics.

Based on the theoretical framework outlined in references [15, 29], it becomes evident that the system described by Eq (2.3) possesses a unique positive global solution. This observation not only confirms the ecological validity of the model but also establishes its mathematical robustness and well-posedness.

As outlined in the introduction, the central focus of this paper revolves around delineating the global threshold that delineates the balance between the sustenance and extinction of zooplankton populations. To address the intricacies posed by the new stochastic system (2.3), we propose a new approach based on the ergodicity of an auxiliary equation closely resembling the equation of y_0. Based

on the stochastic comparison theorem [30], we present the following equation:

$$\begin{cases} \mathrm{d}\tilde{y}_0(t) = \left(\dfrac{r\tilde{y}_0(t)}{s_1r^2 + s_2r + s_3}\left(1 - \dfrac{\tilde{y}_0(t)}{L}\right)\right)\mathrm{d}t + p\displaystyle\sum_{i=0}^{1}\varpi_{0i}\tilde{y}_0^{i+1}(t)\mathrm{d}S_0(t) \\ \qquad\qquad +(1-p)\displaystyle\int_{\mathbb{R}^2\setminus\{0\}}\sum_{j=0}^{1}\nu_{0j}(\xi)\tilde{y}_0^{j+1}(t_-)D_0(\mathrm{d}t,\mathrm{d}\xi), \\ \tilde{y}_0(0) = y_0(0) > 0. \end{cases} \tag{2.5}$$

Based on Lemma 2.2 in [31], it is evident that Eq (2.5) maintains its well-posed nature. Additionally, $\tilde{y}_0(t)$ emerges as a stochastic process endowed with the following properties:

(1) $\mathbb{P}(\tilde{y}_0(t) - y_0(t) \geq 0) = 1$.

(2) If

$$\tilde{d}_0 = \frac{r}{s_1r^2 + s_2r + s_3} - \frac{p^2\varpi_{00}^2}{2} - \int_{\mathbb{R}^2\setminus\{0\}}\Big((1-p)\nu_{00}(\xi) - \log\left(1 + (1-p)\nu_{00}(\xi)\right)\Big)m_0(\mathrm{d}\xi) > 0, \tag{2.6}$$

then there exists a unique ergodic stationary distribution $\tilde{\eta}_0$ for Eq (2.5); and

$$\lim_{t\to\infty}\frac{1}{t}\int_0^t \tilde{y}_0(s)\mathrm{d}s \leq \frac{L\tilde{d}_0}{\left(\frac{r}{s_1r^2+s_2r+s_3} + L(1-p)^2\varpi_{00}\varpi_{01}\right)}.$$

For analytical coherence, it is imperative to maintain the assumption of positivity for $\tilde{d}_0$ throughout this study. Additionally, we rigorously define the following quantities, crucial in delineating the global threshold within the framework of system (2.3):

$$\theta_0 = \alpha e^{\left\{-\frac{1}{\zeta_1}(r-\zeta_2u)^2\right\}}\int_{\mathbb{R}_+} f(y,0)\tilde{\eta}_0(\mathrm{d}y),$$
$$\theta_1 = d_1 + \frac{p^2\varpi_{10}^2}{2} + \int_{\mathbb{R}^2\setminus\{0\}}\Big((1-p)\nu_{10}(\xi) - \log\left(1 + (1-p)\nu_{10}(\xi)\right)\Big)m_0(\mathrm{d}\xi).$$

3. Global threshold of system (2.3)

As elucidated earlier, the crux of ecosystem examination lies in accurately demarcating the threshold that distinguishes between population persistence and decline. Therefore, the paramount aim of the forthcoming theorems is to tackle this pivotal inquiry head-on, while simultaneously enriching our comprehension of algae-zooplankton system dynamics with additional insights and refinements.

Theorem 3.1. *Suppose that $\theta_0 \leq \theta_1$. Under this condition, for any initial positive data $(y_0(0), y_1(0))$, the stochastic system described by Eq (2.3) asymptotically tends towards a state of exponential decline and*

$$\mathbb{P}\left(\lim_{t\to\infty} y_1(t) = 0\right) = 1.$$

Proof. Utilizing Itô's formula, we readily obtain

$$\begin{aligned}
\mathrm{d}\log y_1(t) = &\left(\alpha e^{\left\{-\frac{1}{\zeta_1}(r-\zeta_2 u)^2\right\}} f(y_0(t), y_1(t)) - \beta_1 y_0(t) - d_1 - \frac{p^2}{2}\left(\sum_{i=0}^{1} \varpi_{1i} y_1^i(t)\right)^2\right.\\
&+ \int_{\mathbb{R}^2\setminus\{0\}} \Big(\log\Big(1 + (1-p)\nu_{10}(\xi) + (1-p)\nu_{11}(\xi) y_1(t)\Big) m_1(\mathrm{d}\xi)\\
&\left. - (1-p)\int_{\mathbb{R}^2\setminus\{0\}} \Big(\nu_{10}(\xi) + \nu_{11}(\xi) y_1(t)\Big) m_1(\mathrm{d}\xi)\right)\mathrm{d}t + p\sum_{i=0}^{1} \varpi_{1i} y_1^i(t)\mathrm{d}S_1(t)\\
&+ \int_{\mathbb{R}^2\setminus\{0\}} \log\left(1 + (1-p)\nu_{10}(\xi) + (1-p)\nu_{11}(\xi) y_1(t^-)\right) D_1(\mathrm{d}t, \mathrm{d}\xi).
\end{aligned}$$

In accordance with the stochastic comparison theorem [30], we deduce that

$$\begin{aligned}
\mathrm{d}\log y_1(t) \le &\left(\alpha e^{\left\{-\frac{1}{\zeta_1}(r-\zeta_2 u)^2\right\}} f(\tilde{y}_0(t), 0) - \beta_1 y_0(t) - d_1 - \frac{p^2}{2}\left(\sum_{i=0}^{1} \varpi_{1i} y_1^i(t)\right)^2\right.\\
&+ \int_{\mathbb{R}^2\setminus\{0\}} \Big(\log\Big(1 + (1-p)\nu_{10}(\xi) + (1-p)\nu_{11}(\xi) y_1(t)\Big) m_1(\mathrm{d}\xi)\\
&\left. - (1-p)\int_{\mathbb{R}^2\setminus\{0\}} \Big(\nu_{10}(\xi) + \nu_{11}(\xi) y_1(t)\Big) m_1(\mathrm{d}\xi)\right)\mathrm{d}t + p\sum_{i=0}^{1} \varpi_{1i} y_1^i(t)\mathrm{d}S_1(t)\\
&+ \int_{\mathbb{R}^2\setminus\{0\}} \log\left(1 + (1-p)\nu_{10}(\xi) + (1-p)\nu_{11}(\xi) y_1(t^-)\right) D_1(\mathrm{d}t, \mathrm{d}\xi). \qquad (3.1)
\end{aligned}$$

By integrating the above inequality from 0 to t, we acquire

$$\begin{aligned}
\frac{\log y_1(t)}{t} \le &\frac{\alpha}{t} e^{\left\{-\frac{1}{\zeta_1}(r-\zeta_2 u)^2\right\}} \int_0^t f(\tilde{y}_0(s), 0)\mathrm{d}s - d_1 - \int_{\mathbb{R}^2\setminus\{0\}} \Big((1-p)\nu_{10}(\xi) - \log\left(1 + (1-p)\nu_{10}(\xi)\right)\Big) m_1(\mathrm{d}\xi)\\
&+ \frac{1}{t}\int_0^t \int_{\mathbb{R}^2\setminus\{0\}} \left\{\log\left(1 + \frac{(1-p)\nu_{11}(\xi) y_1(s)}{1 + (1-p)\nu_{10}(\xi)}\right) - (1-p)\nu_{11}(\xi) y_1(s)\right\} m_1(\mathrm{d}\xi)\mathrm{d}s\\
&+ \frac{1}{t}\left(p\int_0^t \sum_{i=0}^{1} \varpi_{1i} y_1^i(s)\mathrm{d}S_2(s) - \frac{p^2}{2}\int_0^t \left(\sum_{i=0}^{1} \varpi_{1i} y_1^i(s)\right)^2 \mathrm{d}s\right)\\
&+ \frac{1}{t}\int_0^t \int_{\mathbb{R}^2\setminus\{0\}} \log\left(1 + (1-p)\nu_{10}(\xi)\right) D_1(\mathrm{d}s, \mathrm{d}\xi) + \frac{\log y_1(0)}{t}\\
&+ \frac{1}{t}\int_0^t \int_{\mathbb{R}^2\setminus\{0\}} \log\left(1 + \frac{(1-p)\nu_{11}(\xi) y_1(s^-)}{1 + (1-p)\nu_{10}(\xi)}\right) D_1(\mathrm{d}s, \mathrm{d}\xi). \qquad (3.2)
\end{aligned}$$

We let $M_0(t) = \displaystyle\int_0^t \int_{\mathbb{R}^2\setminus\{0\}} \log\left(1 + \nu_{10}(\xi)\right) D_1(\mathrm{d}s, \mathrm{d}\xi)$. Then, we get

$$\langle M_0(t), M_0(t)\rangle = t\int_{\mathbb{R}^2\setminus\{0\}} \Big(\log\left(1 + \nu_{10}(\xi)\right)\Big)^2 m_1(\mathrm{d}\xi) < \infty.$$

Referring to the strong law of large numbers, we derive $\mathbb{P}\left(\lim_{t\to\infty}\frac{1}{t}M_0(t)=0\right)=1$. Now, we select $0<\varrho_1<1$ and consider the following quantities:

$$
\begin{aligned}
M_1(t) &= p\int_0^t\sum_{i=0}^{1}\varpi_{1i}y_1^i(s)\mathrm{d}S_1(s)-\frac{p^2}{2}\int_0^t\left(\sum_{i=0}^{1}\varpi_{1i}y_1^i(s)\right)^2\mathrm{d}s,\\
M_2(t) &= p\int_0^t\sum_{i=0}^{1}\varpi_{1i}y_1^i(s)\mathrm{d}S_1(s)-\frac{p^2\varrho_1}{2}\int_0^t\left(\sum_{i=0}^{1}\varpi_{1i}y_1^i(s)\right)^2\mathrm{d}s,\\
M_3(t) &= \int_0^t\int_{\mathbb{R}^2\setminus\{0\}}\left(\left(\frac{(1-p)\nu_{11}(\xi)y_1(s)}{1+(1-p)\nu_{10}(\xi)}\right)+\log\left(1+\frac{(1-p)\nu_{11}(\xi)y_1(s)}{1+(1-p)\nu_{10}(\xi)}\right)\right)m_1(\mathrm{d}\xi)\mathrm{d}s,\\
M_4(t) &= \int_0^t\int_{\mathbb{R}^2\setminus\{0\}}\log\left(1+\frac{(1-p)\nu_{11}(\xi)y_1(s^-)}{1+(1-p)\nu_{10}(\xi)}\right)D_1(\mathrm{d}s,\mathrm{d}\xi).
\end{aligned}
$$

To continue, we employ the exponential inequality designed for martingales, we obtain

$$
\mathbb{P}\left\{\sup_{t\in[0,T_1]}\left(M_2(t)-M_3(t)+M_4(t)\right)>2\varrho_1^{-1}\log\varrho_2\right\}\leq\varrho_2^{-2},\quad\text{for all }\ \varrho_2>0.
$$

Thanks to the Borel-Cantelli lemma, we establish the presence of $\varrho_2(\omega)$ for all $\omega\in\Omega$, ensuring the validity of the following inequality:

$$
p\int_0^t\sum_{i=0}^{1}\varpi_{1i}y_1^i(s)\mathrm{d}S_1(s)+M_4(t)\leq 2\varrho_1^{-1}\log\varrho_2+\frac{p^2\varrho_1}{2}\int_0^t\left(\sum_{i=0}^{1}\varpi_{1i}y_1^i(s)\right)^2\mathrm{d}s+M_3(t),
$$

verifies for any ϱ_2 satisfying $\varrho_2\geq\varrho_2(\omega)$ and $\mathbb{P}(t\in]\varrho_2-1,\varrho_2[)=1$. Consequently,

$$
\begin{aligned}
\frac{M_1(t)}{t}+\frac{M_4(t)}{t} &\leq \frac{2\varrho_1^{-1}\log\varrho_2}{t}+\frac{p^2\varrho_1}{2t}\int_0^t\left(\sum_{i=0}^{1}\varpi_{1i}y_1^i(s)\right)^2\mathrm{d}s-\frac{p^2}{2t}\int_0^t\left(\sum_{i=0}^{1}\varpi_{1i}y_1^i(s)\right)^2\mathrm{d}s\\
&\quad+\frac{1}{t}\int_0^t\int_{\mathbb{R}^2\setminus\{0\}}\left(\left(\frac{(1-p)\nu_{11}(\xi)y_1(s)}{1+(1-p)\nu_{10}(\xi)}\right)-(1-p)\nu_{11}(\xi)y_1(s)\right)m_1(\mathrm{d}\xi)\mathrm{d}s\\
&\leq \frac{2\varrho_1^{-1}\log\varrho_2}{\varrho_2-1}-\frac{p^2(1-\varrho_1)}{2t}\int_0^t\left(\sum_{i=0}^{1}\varpi_{1i}y_1^i(s)\right)^2\mathrm{d}s\\
&\leq \frac{2\varrho_1^{-1}\log\varrho_2}{\varrho_2-1}-\frac{p^2(1-\varrho_1)\varpi_{10}^2}{2}.
\end{aligned}
$$

We compute the upper limit on both sides of Eq (3.2), and then we get

$$
\begin{aligned}
\limsup_{t\to\infty}\frac{\log y_1(t)}{t} &\leq \alpha e^{\left\{-\frac{1}{\zeta_1}(r-\zeta_2u)^2\right\}}\lim_{t\to\infty}\frac{1}{t}\int_0^t f(\tilde{y}_0(s),0)\mathrm{d}s-d_1\\
&\quad-\int_{\mathbb{R}^2\setminus\{0\}}\left((1-p)\nu_{10}(\xi)-\log\left(1+(1-p)\nu_{10}(\xi)\right)\right)m_1(\mathrm{d}\xi)+\lim_{t\to\infty}\frac{1}{t}\phi(t)\\
&\leq \theta_0-d_1-\int_{\mathbb{R}^2\setminus\{0\}}\left((1-p)\nu_{10}(\xi)-\log\left(1+(1-p)\nu_{10}(\xi)\right)\right)m_1(\mathrm{d}\xi)
\end{aligned}
$$

$$+\lim_{\varrho_2\to\infty}\frac{2\varrho_1^{-1}\log\varrho_2}{\varrho_2-1}-\frac{p^2(1-\varrho_1)\varpi_{10}^2}{2}.$$

Therefore,

$$\limsup_{t\to\infty}\frac{\log y_1(t)}{t}\le\theta_0-d_1-\frac{p^2(1-\varrho_1)\varpi_{10}^2}{2}-\int_{\mathbb{R}^2\setminus\{0\}}\Big((1-p)\nu_{10}(\xi)-\log\left(1+(1-p)\nu_{10}(\xi)\right)\Big)m_1(\mathrm{d}\xi).$$

By considering the arbitrary nature of $0<\varrho_1<1$, one can deduce that as ϱ_1 approaches 0,

$$\mathbb{P}\left(\limsup_{t\to\infty}\frac{\log y_1(t)}{t}\le\theta_0-\theta_1<0\right)=1.$$

Put differently, for any arbitrarily small positive quantity $\tilde{\theta}$ satisfying $\tilde{\theta}<\min\{0.5,0.5(\theta_1-\theta_0)\}$, we can infer the existence of $\varrho_3=\varrho_3(\omega)$ associated with Ω_{ϱ_3} such that $\mathbb{P}(\Omega_{\varrho_3})\ge 1-\varrho_3$, where $\log y_1(t)\le -0.5(\theta_1-\theta_0)t$ for all $t\ge\varrho_3$ and $\omega\in\Omega_{\varrho_3}$. As a result, $y_1(t)\le\exp(-0.5(\theta_1-\theta_0)t)$ and

$$\mathbb{P}\left(\limsup_{t\to\infty}y_1(t)\le 0\right)=1.$$

This, coupled with the positivity of the solution (y_0,y_1), suggests

$$\mathbb{P}\left(\lim_{t\to\infty}y_1(t)=0\right)=1.$$

This indicates that the exponential decrease in the population of y_1 implies its almost certain complete eradication. With this, the proof is concluded. □

Corollary 3.1. *(case of second-order Brownian motions) If $p=1$, and*

$$\alpha e^{\left\{-\frac{1}{\zeta_1}(r-\zeta_2u)^2\right\}}\int_{\mathbb{R}_+}f(y,0)\tilde{\eta}_0(\mathrm{d}y)\le d_1+\frac{\varpi_{10}^2}{2},$$

then, the extinction of the population y_1 occurs almost surely.

Corollary 3.2. *(case of second-order jumps) If $p=0$, and*

$$\alpha e^{\left\{-\frac{1}{\zeta_1}(r-\zeta_2u)^2\right\}}\int_{\mathbb{R}_+}f(y,0)\tilde{\eta}_0(\mathrm{d}y)\le d_1+\int_{\mathbb{R}^2\setminus\{0\}}\Big(\nu_{10}(\xi)-\log\left(1+\nu_{10}(\xi)\right)\Big)m_0(\mathrm{d}\xi),$$

then, the extinction of the population y_1 occurs almost surely.

Theorem 3.2. *Suppose that $\theta_0>\theta_1$. Under this condition, for any initial positive data $(y_0(0),y_1(0))$, the stochastic system described by Eq* (2.3) *asymptotically tends towards a stationary state and*

$$\mathbb{P}\left(\liminf_{t\to\infty}\frac{1}{t}\int_0^t y_\ell(s)\mathrm{d}s=\int_{\mathbb{R}_+^2}y_\ell\eta(y_0,y_1)>0\right)=1,\quad\forall\ell=0,1,$$

where $\eta(\cdot,\cdot)$ is the unique ergodic stationary distribution associated with system (2.3).

Proof. Utilizing the Itô formula for the function $F_0(t) = \log\left(\frac{\tilde{y}_0(t)}{y_0(t)}\right)$ yields:

$$\begin{aligned}\mathcal{L}F_0(t) \leq & -\frac{r}{L(s_1r^2+s_2r+s_3)}\Big(\tilde{y}_0(t)-y_0(t)\Big)+\frac{1}{y_0(t)}e^{\left\{-\frac{1}{\zeta_1}(r-\zeta_2u)^2\right\}}f(y_0(t),y_1(t))y_1(t)\\ & -\frac{1}{2}\left(p\sum_{i=0}^{1}\varpi_{0i}\tilde{y}_0^i(t)\right)^2+\frac{1}{2}\left(p\sum_{i=0}^{1}\varpi_{0i}y_0^i(t)\right)^2\\ & +\int_{\mathbb{R}^2\setminus\{0\}}\Big\{\log\Big(\frac{1+(1-p)\nu_{00}(\xi)+(1-p)\nu_{01}(\xi)\tilde{y}_0(t)}{1+(1-p)\nu_{00}(\xi)+(1-p)\nu_{01}(\xi)y_0(t)}\Big)-(1-p)\nu_{01}(\xi)(\tilde{y}_0(t)-y_0(t))\Big\}m_0(\mathrm{d}\xi).\end{aligned}$$

Based on the properties of the function f, it follows that:

$$\begin{aligned}\mathcal{L}F_0(t) \leq & -\frac{r}{L(s_1r^2+s_2r+s_3)}\Big(\tilde{y}_0(t)-y_0(t)\Big)+\vartheta e^{\left\{-\frac{1}{\zeta_1}(r-\zeta_2u)^2\right\}}y_1(t)\\ & -(\tilde{y}_0(t)-y_0(t))\int_{\mathbb{R}^2\setminus\{0\}}\Big\{\frac{(1-p)^2\nu_{01}(\xi)(\nu_{00}(\xi)+\nu_{01}(\xi)y_0(t))}{1+(1-p)\nu_{00}(\xi)+(1-p)\nu_{01}(\xi)y_0(t)}\Big\}m_0(\mathrm{d}\xi).\end{aligned}$$

By virtue of the positive property of the solution, we obtain:

$$\mathcal{L}F_0(t) \leq -\frac{r}{L(s_1r^2+s_2r+s_3)}\Big(\tilde{y}_0(t)-y_0(t)\Big)+\vartheta e^{\left\{-\frac{1}{\zeta_1}(r-\zeta_2u)^2\right\}}y_1(t). \tag{3.3}$$

Once more, employing the operator $\mathcal{L}$ on the second equation of (2.3) yields:

$$\begin{aligned}\mathcal{L}\log\left(\frac{1}{y_1(t)}\right) = & -\alpha e^{\left\{-\frac{1}{\zeta_1}(r-\zeta_2u)^2\right\}}f(y_0(t),y_1(t))+\beta_1y_0(t)+d_1+\frac{1}{2}\left(p\sum_{i=0}^{1}\varpi_{1i}y_1^i(t)\right)^2\\ & -\int_{\mathbb{R}^2\setminus\{0\}}\Big\{\log\Big(1+(1-p)\nu_{10}(\xi)+(1-p)\nu_{11}(\xi)y_1(t)\Big)\\ & -(1-p)\Big(\nu_{10}(\xi)+\nu_{11}(\xi)y_1(t)\Big)\Big\}m_1(\mathrm{d}\xi).\end{aligned}$$

Consequently,

$$\begin{aligned}\mathcal{L}\log\left(\frac{1}{y_1(t)}\right) = & -\alpha e^{\left\{-\frac{1}{\zeta_1}(r-\zeta_2u)^2\right\}}f(\tilde{y}_0(t),0)+\beta_1y_0(t)+d_1+\frac{p^2\varpi_{10}^2}{2}\\ & +\int_{\mathbb{R}^2\setminus\{0\}}\Big((1-p)\nu_{10}(\xi)-\log\left(1+(1-p)\nu_{10}(\xi)\right)\Big)m_1(\mathrm{d}\xi)\\ & +\alpha e^{\left\{-\frac{1}{\zeta_1}(r-\zeta_2u)^2\right\}}f(\tilde{y}_0(t),0)-\alpha e^{\left\{-\frac{1}{\zeta_1}(r-\zeta_2u)^2\right\}}f(y_0(t),y_1(t))-\alpha e^{\left\{-\frac{1}{\zeta_1}(r-\zeta_2u)^2\right\}}f(y_0(t),0)\\ & +\alpha e^{\left\{-\frac{1}{\zeta_1}(r-\zeta_2u)^2\right\}}f(y_0(t),0)+p\varpi_{10}\varpi_{11}y_1(t)+\frac{p^2}{2}\varpi_{11}^2y_1^2(t)\\ & +\int_{\mathbb{R}^2\setminus\{0\}}\Big\{(1-p)\nu_{11}(\xi)y_1(t)-\log\Big(1+\frac{(1-p)\nu_{11}(\xi)y_1(t)}{1+(1-p)\nu_{10}(\xi)}\Big)\Big\}m_1(\mathrm{d}\xi).\end{aligned}$$

Consistent with the positivity of the solution, we find

$$\mathcal{L}\log\left(\frac{1}{y_1(t)}\right) \leq -\alpha e^{\left\{-\frac{1}{\zeta_1}(r-\zeta_2u)^2\right\}}f(\tilde{y}_0(t),0)+d_1+\frac{p^2\varpi_{10}^2}{2}$$

$$
\begin{aligned}
&+ \int_{\mathbb{R}^2\setminus\{0\}} \Big((1-p)\nu_{10}(\xi) - \log\left(1+(1-p)\nu_{10}(\xi)\right)\Big) m_1(\mathrm{d}\xi) \\
&+ \beta_1 y_0(t) + \alpha\vartheta e^{\left\{-\frac{1}{\zeta_1}(r-\zeta_2 u)^2\right\}}(\tilde{y}_0(t) - y_0(t)) \\
&+ \left(p\varpi_{10}\varpi_{11} + (1-p)\int_{\mathbb{R}^2\setminus\{0\}} \nu_{11}(\xi) m_0(\mathrm{d}\xi)\right) y_1(t) \\
&+ \frac{p^2}{2}\varpi_{11}^2 y_1^2(t) + \alpha e^{\left\{-\frac{1}{\zeta_1}(r-\zeta_2 u)^2\right\}} f(y_0(t),0) - \alpha e^{\left\{-\frac{1}{\zeta_1}(r-\zeta_2 u)^2\right\}} f(y_0(t), y_1(t)).
\end{aligned} \tag{3.4}
$$

Now, let us examine the following function:

$$
F_1(t) = \frac{L\alpha\vartheta}{r}(s_1 r^2 + s_2 r + s_3) e^{\left\{-\frac{1}{\zeta_1}(r-\zeta_2 u)^2\right\}} F_0(t) + \log\left(\frac{1}{y_1(t)}\right).
$$

By applying the operator $\mathcal{L}$ to F_1, we obtain

$$
\begin{aligned}
\mathcal{L}F_1(t) \leq\ & -\alpha e^{\left\{-\frac{1}{\zeta_1}(r-\zeta_2 u)^2\right\}} f(\tilde{y}_0(t),0) + d_1 + \frac{p^2\varpi_{10}^2}{2} \\
&+ \int_{\mathbb{R}^2\setminus\{0\}} \Big((1-p)\nu_{10}(\xi) - \log\left(1+(1-p)\nu_{10}(\xi)\right)\Big) m_1(\mathrm{d}\xi) \\
&+ \beta_1 y_0(t) + \left(p\varpi_{10}\varpi_{11} + (1-p)\int_{\mathbb{R}^2\setminus\{0\}} \nu_{11}(\xi) m_0(\mathrm{d}\xi)\right) y_1(t) \\
&+ \frac{L(s_1 r^2 + s_2 r + s_3)\alpha\vartheta^2}{r} e^{2\left\{-\frac{1}{\zeta_1}(r-\zeta_2 u)^2\right\}} y_1(t) \\
&+ \alpha e^{\left\{-\frac{1}{\zeta_1}(r-\zeta_2 u)^2\right\}} f(y_0(t),0) - \alpha e^{\left\{-\frac{1}{\zeta_1}(r-\zeta_2 u)^2\right\}} f(y_0(t), y_1(t)) + \frac{p^2}{2}\varpi_{11}^2 y_1^2(t).
\end{aligned}
$$

By rearranging certain terms, we achieve

$$
\begin{aligned}
\mathcal{L}F_1(t) \leq\ & -\alpha e^{\left\{-\frac{1}{\zeta_1}(r-\zeta_2 u)^2\right\}} \int_{\mathbb{R}_+} f(y,0)\tilde{\eta}_0(\mathrm{d}y) + d_1 + \frac{p^2\varpi_{10}^2}{2} \\
&+ \int_{\mathbb{R}^2\setminus\{0\}} \Big((1-p)\nu_{10}(\xi) - \log\left(1+(1-p)\nu_{10}(\xi)\right)\Big) m_1(\mathrm{d}\xi) \\
&+ \beta_1 y_0(t) + \frac{p^2}{2}\varpi_{11}^2 y_1^2(t) + \alpha e^{\left\{-\frac{1}{\zeta_1}(r-\zeta_2 u)^2\right\}} \left(\int_{\mathbb{R}_+} f(y,0)\tilde{\eta}_0(\mathrm{d}y) - f(\tilde{y}_0(t),0)\right) \\
&+ \left(\frac{L(s_1 r^2 + s_2 r + s_3)\alpha\vartheta^2}{r} e^{2\left\{-\frac{1}{\zeta_1}(r-\zeta_2 u)^2\right\}} + p\varpi_{10}\varpi_{11} + (1-p)\int_{\mathbb{R}^2\setminus\{0\}} \nu_{11}(\xi) m_0(\mathrm{d}\xi)\right) y_1(t) \\
&+ \alpha e^{\left\{-\frac{1}{\zeta_1}(r-\zeta_2 u)^2\right\}} f(y_0(t),0) - \alpha e^{\left\{-\frac{1}{\zeta_1}(r-\zeta_2 u)^2\right\}} f(y_0(t), y_1(t)).
\end{aligned}
$$

Once more, let us examine this new function:

$$
F_2(t) = F_1(t) + c_\star y_1(t).
$$

Here, $c_\star$ denotes a positive constant that fulfills:

$$
c_\star \geq \frac{1}{d_1}\left(\frac{L(s_1 r^2 + s_2 r + s_3)\alpha\vartheta^2}{r} e^{2\left\{-\frac{1}{\zeta_1}(r-\zeta_2 u)^2\right\}} + p\varpi_{10}\varpi_{11} + (1-p)\int_{\mathbb{R}^2\setminus\{0\}} \nu_{11}(\xi) m_1(\mathrm{d}\xi)\right).
$$

Upon applying the operator $\mathcal{L}$ to F_2, we acquire

$$\begin{aligned}\mathcal{L}F_2(t) \leq & -\alpha e^{\left\{-\frac{1}{\zeta_1}(r-\zeta_2 u)^2\right\}} \int_{\mathbb{R}_+} f(y,0)\tilde{\eta}_0(\mathrm{d}y) + d_1 + \frac{p^2\varpi_{10}^2}{2} \\ & + \int_{\mathbb{R}^2\setminus\{0\}} \Big((1-p)\nu_{10}(\xi) - \log\left(1+(1-p)\nu_{10}(\xi)\right)\Big) m_1(\mathrm{d}\xi) \\ & + \alpha e^{\left\{-\frac{1}{\zeta_1}(r-\zeta_2 u)^2\right\}} \Big(\int_{\mathbb{R}_+} f(y,0)\tilde{\eta}_0(\mathrm{d}y) - f(\tilde{y}_0(t),0)\Big) + \alpha e^{\left\{-\frac{1}{\zeta_1}(r-\zeta_2 u)^2\right\}} f(y_0(t),0) \\ & - \alpha e^{\left\{-\frac{1}{\zeta_1}(r-\zeta_2 u)^2\right\}} f(y_0(t),y_1(t)) + \beta_1 y_0(t) + \frac{p^2}{2}\varpi_{11}^2 y_1^2(t) + c_\star \alpha e^{\left\{-\frac{1}{\zeta_1}(r-\zeta_2 u)^2\right\}} f(y_0(t),y_1(t))y_1(t).\end{aligned}$$

Then

$$\begin{aligned}\mathcal{L}F_2(t) \leq & \ \theta_1 - \theta_0 + \alpha e^{\left\{-\frac{1}{\zeta_1}(r-\zeta_2 u)^2\right\}} \Big(\int_{\mathbb{R}_+} f(x,0)\tilde{\eta}_0(\mathrm{d}x) - f(\tilde{y}_0(t),0)\Big) \\ & + \alpha e^{\left\{-\frac{1}{\zeta_1}(r-\zeta_2 u)^2\right\}} \Big(f(y_0(t),0) - f(y_0(t),y_1(t))\Big) \\ & + \beta_1 y_0(t) + \frac{p^2}{2}\varpi_{11}^2 y_1^2(t) + c_\star \alpha e^{\left\{-\frac{1}{\zeta_1}(r-\zeta_2 u)^2\right\}} f(y_0(t),y_1(t))y_1(t).\end{aligned}$$

Let $c_{\star\star} \in (0,1)$, then we define a new function as follows:

$$F_3(t) = \frac{1}{c_{\star\star}}(y_0^{c_{\star\star}}(t) + y_1^{c_{\star\star}}(t)).$$

By applying the operator $\mathcal{L}$ to F_3, we get

$$\begin{aligned}\mathcal{L}F_3(t) = & \ y_0^{c_{\star\star}-1}(t)\left\{\frac{ry_0(t)}{s_1r^2+s_2r+s_3}\left(1-\frac{y_0(t)}{\mathcal{L}}\right) - e^{\left\{-\frac{1}{\zeta_1}(r-\zeta_2 u)^2\right\}} f(y_0(t),y_1(t))y_1(t)\right\} \\ & + \frac{(c_{\star\star}-1)}{2} y_0^{c_{\star\star}-2}(t)\left(p\sum_{i=0}^{1}\varpi_{0i}y_0^{i+1}(t)\right)^2 \\ & + \int_{\mathbb{R}^2\setminus\{0\}} \left\{\frac{\left(y_0(t)+(1-p)\nu_{00}(\xi)y_0(t)+(1-p)\nu_{01}(\xi)y_0^2(t)\right)^{c_{\star\star}}}{c_{\star\star}} - \frac{y_0^{c_{\star\star}}(t)}{c_{\star\star}}\right\} m_0(\mathrm{d}\xi) \\ & - \int_{\mathbb{R}^2\setminus\{0\}} (1-p)y_0^{c_{\star\star}-1}(t)(\nu_{00}(\xi)y_0(t)+\nu_{01}(\xi)y_0^2(t))m_0(\mathrm{d}\xi) \\ & + y_1^{c_{\star\star}-1}(t)\Big(\alpha e^{\left\{-\frac{1}{\zeta_1}(r-\zeta_2 u)^2\right\}} f(y_0(t),y_1(t))y_1(t) - \beta y_0(t)y_1(t) - d_1 y_1(t)\Big) \\ & + \frac{(c_{\star\star}-1)}{2} y_1^{c_{\star\star}-2}(t)\left(p\sum_{i=0}^{1}\varpi_{1i}y_1^{i+1}(t)\right)^2 \\ & + \int_{\mathbb{R}^2\setminus\{0\}} \left(\frac{\left(y_1(t)+(1-p)\nu_{10}(\xi)y_1(t)+(1-p)\nu_{11}(\xi)y_1^2(t)\right)^{c_{\star\star}}}{c_{\star\star}} - \frac{y_1^{c_{\star\star}}(t)}{c_{\star\star}}\right) m_1(\mathrm{d}\xi) \\ & - \int_{\mathbb{R}^2\setminus\{0\}} (1-p)y_1^{c_{\star\star}}(t)(\nu_{00}(\xi)+\nu_{01}(\xi)y_1(t))m_0(\mathrm{d}\xi)\end{aligned}$$

$$\leq \frac{r}{s_1 r^2 + s_2 r + s_3} y_0^{c_{\star\star}}(t) - \frac{(1-c_{\star\star})}{2}\varpi_{01}^2 y_0^{c_{\star\star}+2}(t) + \frac{\alpha e^{\left\{-\frac{1}{\zeta_1}(r-\zeta_2 u)^2\right\}}\vartheta}{c_{\star\star}+1} y_0^{c_{\star\star}+1}(t)$$
$$+ \frac{\alpha c_{\star\star} e^{\left\{-\frac{1}{\zeta_1}(r-\zeta_2 u)^2\right\}}\vartheta}{c_{\star\star}+1} y_1^{c_{\star\star}+1}(t) - \frac{(1-c_{\star\star})}{2}\varpi_{11}^2 y_1^{c_{\star\star}+2}(t).$$

We amalgamate functions F_2 and F_3 in the following manner:

$$F_4(t) = h_\star F_2(t) + F_3(t).$$

Here, $h_\star > 0$ satisfies $2 + \mathcal{K}_\star - h_\star(\overbrace{\theta_0 - \theta_1}^{>0}) \leq 0$, where $\mathcal{K}_\star = \max\{\mathcal{A}_\star, 1\}$, and

$$\mathcal{A}_\star = \sup_{(y_0,y_1)\in\mathbb{R}^2_{o,+}} \Big\{ \frac{r}{s_1 r^2 + s_2 r + s_3} y_0^{c_{\star\star}}(t) - \frac{(1-c_{\star\star})}{4}\varpi_{01}^2 y_0^{c_{\star\star}+2}(t) + \frac{\alpha e^{\left\{-\frac{1}{\zeta_1}(r-\zeta_2 u)^2\right\}}\vartheta}{c_{\star\star}+1} y_0^{c_{\star\star}+1}(t)$$
$$+ \frac{\alpha c_{\star\star} e^{\left\{-\frac{1}{\zeta_1}(r-\zeta_2 u)^2\right\}}\vartheta}{c_{\star\star}+1} y_1^{c_{\star\star}+1}(t) - \frac{(1-c_{\star\star})}{4}\varpi_{11}^2 y_1^{c_{\star\star}+2}(t)\Big\}.$$

To guarantee the positivity of our Lyapunov function, we introduce this new function:

$$F_5(t) = F_4(t) - \underline{F}_4,$$

where, $\underline{F}_4$ represents the lower bound of function F_4. When we apply the operator $\mathcal{L}$ to F_5, we obtain

$$\mathcal{L}F_5(t) \leq F_6(t) + h_\star \alpha e^{\left\{-\frac{1}{\zeta_1}(r-\zeta_2 u)^2\right\}}\Big(\int_{\mathbb{R}_+} f(y,0)\tilde{\eta}_0(\mathrm{d}y) - f(\tilde{y}_0(t),0)\Big), \tag{3.5}$$

where

$$F_6(t) = h_\star(\overbrace{\theta_1 - \theta_0}^{<0}) + h_\star c_\star \alpha e^{\left\{-\frac{1}{\zeta_1}(r-\zeta_2 u)^2\right\}}\vartheta y_0(t) y_1(t) + \beta_1 y_0(t) + h_\star \frac{p^2}{2}\varpi_{11}^2 y_1^2(t)$$
$$+ \frac{r}{s_1 r^2 + s_2 r + s_3} y_0^{c_{\star\star}}(t) - \frac{(1-c_{\star\star})}{4}\varpi_{01}^2 y_0^{c_{\star\star}+2}(t) + \frac{\alpha e^{\left\{-\frac{1}{\zeta_1}(r-\zeta_2 u)^2\right\}}\vartheta}{c_{\star\star}+1} y_0^{c_{\star\star}+1}(t)$$
$$+ \frac{\alpha c_{\star\star} e^{\left\{-\frac{1}{\zeta_1}(r-\zeta_2 u)^2\right\}}\vartheta}{c_{\star\star}+1} y_1^{c_{\star\star}+1}(t) - \frac{(1-c_{\star\star})}{4}\varpi_{11}^2 y_1^{c_{\star\star}+2}(t).$$

Utilizing the methodologies outlined in the proof of Theorem 3.2 in [31], along with the properties of the function f, we can promptly verify $F_6(t) \leq -1$, $\forall (y_0, y_1) \in \mathbb{R}^2_+ \setminus H_x = H_x^c$, $x > 0$, where

$$H_x = \Big\{(y_0, y_1) \in \mathbb{R}^2_+ |\ \ x \leq y_0 \leq x^{-1}, \quad x \leq y_1 \leq x^{-1}\Big\}.$$

Alternatively, it's evident that there exists a positive constant κ such that $F_6(t) \leq \kappa$ for all $(y_0, y_1) \in H_x$. Then, from (3.5), we derive

$$0 \leq \int_0^t \mathbb{E}F_6(t)\mathrm{d}s + h_\star \alpha e^{\left\{-\frac{1}{\zeta_1}(r-\zeta_2 u)^2\right\}} \times \mathbb{E}\Big(\int_0^t \int_{\mathbb{R}_+} f(y,0)\tilde{\eta}_0(\mathrm{d}y)\mathrm{d}s - \int_0^t f(\tilde{y}_0(s),0)\mathrm{d}s\Big).$$

By virtue of the ergodicity property of the process $\tilde{y}$, we obtain

$$0 \leq \liminf_{t\to\infty} \frac{1}{t} \int_0^t \Big(\mathbb{E}F_6(t)\mathbb{1}_{\{(y_0,y_1)\in H_x\}} + \mathbb{E}F_6(t)\mathbb{1}_{\{(y_0,y_1)\in H_x^c\}}\Big)\mathrm{d}s.$$

So,

$$\begin{aligned} 0 &\leq \liminf_{t\to\infty} \frac{1}{t} \int_0^t \Big(\kappa\mathbb{P}((y_0,y_1)\in H_x) - \mathbb{P}((y_0,y_1)\in H_x^c)\Big)\mathrm{d}s \\ &= \liminf_{t\to\infty} \frac{1}{t} \int_0^t \Big(\kappa\mathbb{P}((y_0,y_1)\in H_x) - 1 + \mathbb{P}((y_0,y_1)\in H_x)\Big)\mathrm{d}s. \end{aligned}$$

Consequently,

$$\liminf_{t\to\infty} \frac{1}{t} \int_0^t \mathbb{P}((y_0,y_1)\in H_x)\mathrm{d}s \geq (1+\kappa)^{-1} > 0.$$

By employing the lemma of mutually constrained possibilities [32], we infer the existence of a unique ergodic stationary distribution $\eta(\cdot,\cdot)$. Hence, incorporating the ergodic property into consideration, we can firmly conclude that

$$\begin{aligned} \mathbb{P}\left(\liminf_{t\to\infty} \frac{1}{t} \int_0^t y_0(s)\mathrm{d}s = \int_{\mathbb{R}_+^2} y_0\eta(y_0,y_1) > 0\right) = 1, \\ \mathbb{P}\left(\liminf_{t\to\infty} \frac{1}{t} \int_0^t y_1(s)\mathrm{d}s = \int_{\mathbb{R}_+^2} y_1\eta(y_0,y_1) > 0\right) = 1. \end{aligned}$$

This implies that the system asymptotically converges to the persistent state over time. Thus, the proof is concluded. □

Corollary 3.3. *(case of second-order Brownian motions) If $p = 1$, and*

$$\alpha e^{\left\{-\frac{1}{\zeta_1}(r-\zeta_2 u)^2\right\}} \int_{\mathbb{R}_+} f(y,0)\tilde{\eta}_0(\mathrm{d}y) > d_1 + \frac{\varpi_{10}^2}{2},$$

then, the permanence of the populations y_1 and y_1 occurs almost surely.

Corollary 3.4. *(case of second-order jumps) If $p = 0$, and*

$$\alpha e^{\left\{-\frac{1}{\zeta_1}(r-\zeta_2 u)^2\right\}} \int_{\mathbb{R}_+} f(y,0)\tilde{\eta}_0(\mathrm{d}y) > d_1 + \int_{\mathbb{R}^2\setminus\{0\}} \Big(\nu_{10}(\xi) - \log\left(1+\nu_{10}(\xi)\right)\Big)m_0(\mathrm{d}\xi),$$

then, the permanence of the populations y_1 and y_1 occurs almost surely.

Remark 3.1. *From Theorem 3.1, we infer that the zooplankton population tends to extinction rapidly. This rapid decline suggests that under certain conditions, the zooplankton cannot sustain its population over time, likely due to insufficient resources, high predation pressure, or adverse environmental factors. The extinction of zooplankton can disrupt the balance of the aquatic ecosystem, affecting nutrient cycling and the food web structure. In contrast, Theorem 3.2 implies the persistence and stationarity of both algae and zooplankton populations. This means that under a different set of conditions, both populations are able to maintain stable levels over time, without the risk of extinction. The persistence of these populations indicates a balanced interaction between the species, where the growth rates of algae and zooplankton, along with other ecological factors, allow for long-term coexistence.*

4. Numerical application and discussion

In this section, we carry out a series of numerical examples to validate the findings presented in our study, utilizing the data outlined in [14]. We take $r = 0.3$, $u = 0.25$, $s_1 = 0.02$, $s_2 = 0.02$, $s_3 = 0.08$, $L = (2.5; 3.5)$, $\zeta_1 = 2$, $\zeta_2 = 0.5$, $\alpha = 0.4, \beta_1 = 0.2$, and $d_1 = 0.6$. About the dual incidence functions g_1 and g_2, we consider the following general nonlinear incidence:

$$f(y_0, y_1) = \frac{\beta_0 y_0}{1 + k_0 y_0 + k_1 y_1 + k_2 y_0 y_1},$$

where $\beta_0 = 4.5$, $k_0 = 0.16$, $k_0 = 0.11$ and $k_2 = 0.012$. To simulate the stochastic component, we present a method for simulating jumps and tempered stable processes [28]. Firstly, we examine the sequences $\{S_{1,j}\}_{j\geqslant 1}$, $\{S_{2,j}\}_{j\geqslant 1}$, and $\{S_{3,j}\}_{j\geqslant 1}$, representing independent and identically distributed (i.i.d.) random variables taking values in the real numbers, following the distribution (2.4). Additionally, we define $\{S_{2,j}\}_{j\geqslant 1}$ and $\{S_{3,j}\}_{j\geqslant 1}$ as i.i.d. sequences of uniform random variables within the intervals $(0, 1)$ and $(0, T)$, respectively. Furthermore, consider $\{S_{4,j}\}_{j\geqslant 1}$ and $\{S_{5,j}\}_{j\geqslant 1}$ as i.i.d. sequences of random variables following an exponential distribution with a rate coefficient of 1. It is assumed that all the aforementioned random variables are mutually independent. Then, we let $\{S_{6,j}\} = \sum_{k=1}^{j} \{S_{5,k}\}$. Noticeably, $\{S_{6,j}\}$ can be regarded as a Poisson point process on the interval $\mathbb{R}_+$ with random intensity measure. In reference to the theory outlined in [28], if $\alpha_s \in (0, 2)$, then

$$m_t = \sum_{j=1}^{+\infty} \frac{S_{1,j} \mathbf{1}_{\{S_{3,j} \leqslant t\}}}{|S_{1,j}|} \left(\left(\frac{\alpha_s S_{6,j}}{T \|\rho\|} \right)^{\alpha_s^{-1}} \wedge \left(\frac{S_{2,j}^{\alpha_s^{-1}} S_{4,j}}{|S_{1,j}|} \right) \right),$$

converges almost surely and uniformly for t within the interval $[0, T]$ to a Lévy process, where $\|\rho\| = \int_{\mathbb{R}^2 \setminus \{0\}} |x|^{\alpha_s} R_k(\mathrm{d}x)$. In practice, we can devise a method for generating a jump process with specified parameters at discrete time instances t_i. Here, $t_{i i \in [0,I]}$ denotes a partition of the interval $[0, T]$, characterized by uniformly sized sub-intervals and a mesh size $\Delta t = T/I$, where $I \in \mathbb{N}$. Subsequently, we employ the following algorithm:

(1) Choose a specific time duration, denoted as T, and partition the time interval $[0, T]$ into I equal-sized segments.

(2) Specify and fix a numerical parameter, denoted as N.

(3) Generate numerical replications or simulations of independent quantities $S_{i,j}$, where i ranges from 1 to 6, with a sample size of N.

(4) Calculate the value of m_t.

Let us now direct our attention to the following system:

$$\begin{cases} \mathrm{d}y_0(t) = \left(\dfrac{ry_0(t)}{s_1r^2 + s_2r + s_3}\left(1 - \dfrac{y_0(t)}{L}\right) - \dfrac{\beta_0 y_0(t)y_1(t)e^{\left\{-\frac{1}{\zeta_1}(r-\zeta_2 u)^2\right\}}}{1 + k_0y_0(t) + k_1y_1(t) + k_2y_0(t)y_1(t)} \right)\mathrm{d}t \\ \qquad\quad + p\sum_{i=0}^{1}\varpi_{0i}y_0^{i+1}(t)\mathrm{d}S_0(t) + (1-p)\int_{\mathbb{R}^2\setminus\{0\}}\sum_{j=0}^{1}\nu_{0j}(\xi)y_0^{j+1}(t_-)D_0(\mathrm{d}t,\mathrm{d}\xi), \\ \mathrm{d}y_1(t) = \left(\dfrac{\alpha\beta_0 y_0(t)y_1(t)e^{\left\{-\frac{1}{\zeta_1}(r-\zeta_2 u)^2\right\}}}{1 + k_0y_0(t) + k_1y_1(t) + k_2y_0(t)y_1(t)} - \beta_1 y_0(t)y_1(t) - d_1y_1(t) \right)\mathrm{d}t \\ \qquad\quad + p\sum_{i=0}^{1}\varpi_{1i}y_1^{i+1}(t)\mathrm{d}S_1(t) + (1-p)\int_{\mathbb{R}^2\setminus\{0\}}\sum_{j=0}^{1}\nu_{1j}(\xi)y_1^{j+1}(t_-)D_1(\mathrm{d}t,\mathrm{d}\xi), \\ y_0(0) = 2.5, \quad y_1(0) = 1.8. \end{cases} \tag{4.1}$$

By incorporating the ergodic property of Eq (2.5), we define the parameters θ_0 and θ_1 as follows:

$$\theta_0 = \int_{\mathbb{R}_+}\frac{\alpha\beta_0 y e^{\left\{-\frac{1}{\zeta_1}(r-\zeta_2 u)^2\right\}}}{1 + k_1y}\tilde{\eta}_0(\mathrm{d}y) = \lim_{t\to\infty}\frac{1}{t}\int_0^t \frac{\alpha\beta_0 e^{\left\{-\frac{1}{\zeta_1}(r-\zeta_2 u)^2\right\}}\tilde{y}_0(s)}{1 + k_0\tilde{y}_0(s)}\mathrm{d}s,$$

$$\theta_1 = d_1 + \frac{p^2\varpi_{10}^2}{2} + \int_{\mathbb{R}^2\setminus\{0\}}\Big((1-p)\nu_{10}(\xi) - \log\left(1 + (1-p)\nu_{10}(\xi)\right)\Big)m_0(\mathrm{d}\xi).$$

4.1. Case 1: Almost sure extinction of y_1

Firstly, we consider $L = 2.5$, $p = 0.5$ and we take the noise parameters as follows: $\varpi_{00} = 0.02$, $\varpi_{01} = 0.01$, $\varpi_{10} = 0.021$, $\varpi_{11} = 0.012$, $\nu_{00} = 0.01$, $\nu_{01} = 0.009$, $\nu_{10} = 0.02$ and $\nu_{11} = 0.007$. In this case, we get $\theta_1 = 0.0526$ and $\theta_2 = 0.07492$. According to Theorem 3.1, it is highly probable that the population y_1 will become extinct. This outcome is visually exemplified in Figure 1, which provides a numerical illustration of the aforementioned result.

Secondly, we take $p = 1$ and we establish specific values for the white noise parameters $\varpi_{00} = 0.02$, $\varpi_{01} = 0.01$, $\varpi_{10} = 0.021$ and $\varpi_{11} = 0.012$. In this case, we get $\theta_1 = 0.0526$ and $\theta_2 = 0.1894$. As a result, we have verified that the prerequisite outlined in Corollary 3.1 has been met and the extinction of y_1 occurs almost surely. This result is visually depicted in Figure 2.

Now, we set $p = 0$. The jump intensities are defined as follows: $\nu_{00} = 0.01$, $\nu_{01} = 0.009$, $\nu_{10} = 0.02$ and $\nu_{11} = 0.007$. Here, we get $\theta_1 = 0.0526$ and $\theta_2 = 0.118$. As a result, we have verified that the prerequisite outlined in Corollary 3.2 has been met. This result is visually depicted in Figure 3.

Upon scrutinizing the aforementioned figures, a discernible pattern emerges: The extinction time is contingent upon the nature of the noise. Notably, a significant presence of noise hastens the extinction process considerably. This observation underscores the critical influence of noise intensity on the dynamics of extinction within the system.

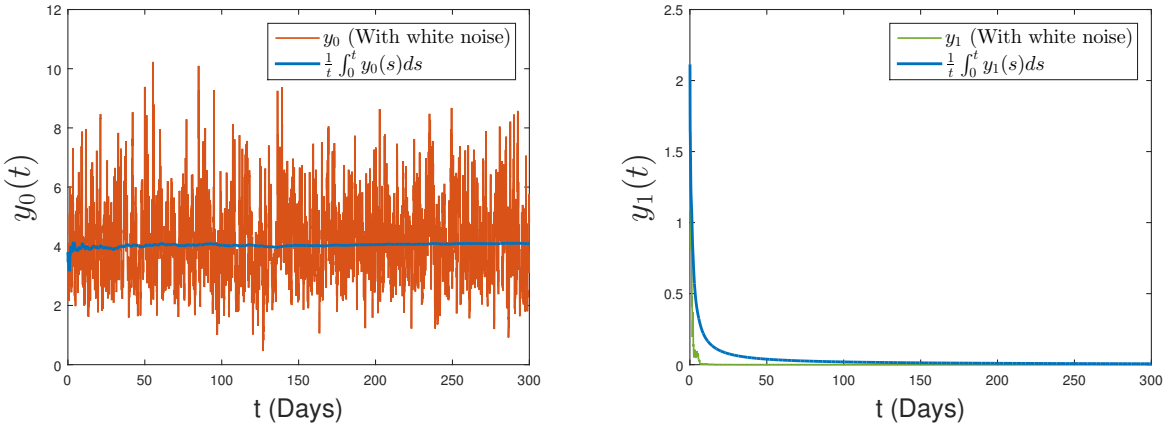

Figure 1. Conducting numerical simulations for solving system (4.1) in the presence of second-order noise. In this case, we take $L = 2.5$ and $p = 0.5$. The white noise parameters are selected as follows: $\varpi_{00} = 0.02$, $\varpi_{01} = 0.01$, $\varpi_{10} = 0.021$ and $\varpi_{11} = 0.012$. The jump intensities are defined as follows: $\nu_{00} = 0.01$, $\nu_{01} = 0.009$, $\nu_{10} = 0.02$ and $\nu_{11} = 0.007$. Here, we get $\theta_1 = 0.0526$ and $\theta_2 = 0.118$.

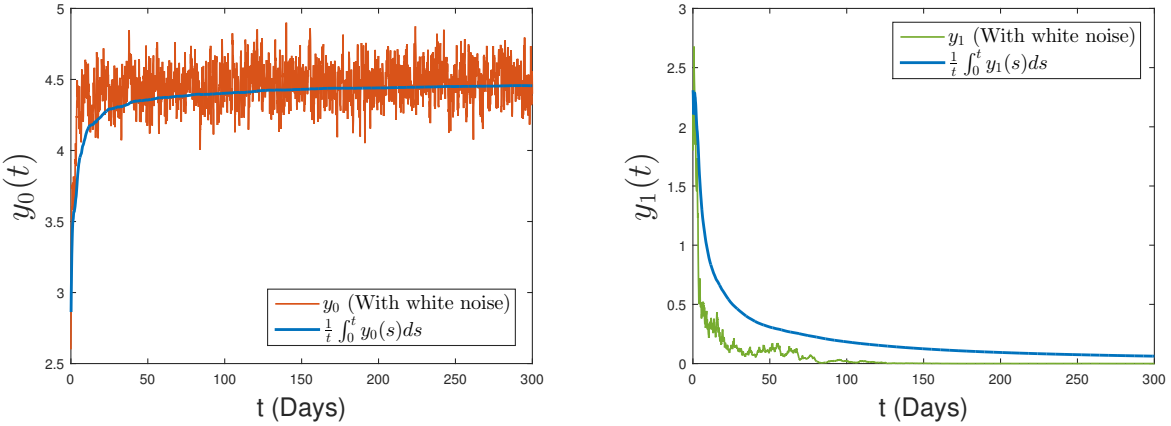

Figure 2. Conducting numerical simulations for solving system (4.1) in the presence of second-order white noise. In this case, we take $L = 2.5$ and $p = 1$. The white noise parameters are selected as follows: $\varpi_{00} = 0.02$, $\varpi_{01} = 0.01$, $\varpi_{10} = 0.021$ and $\varpi_{11} = 0.012$.

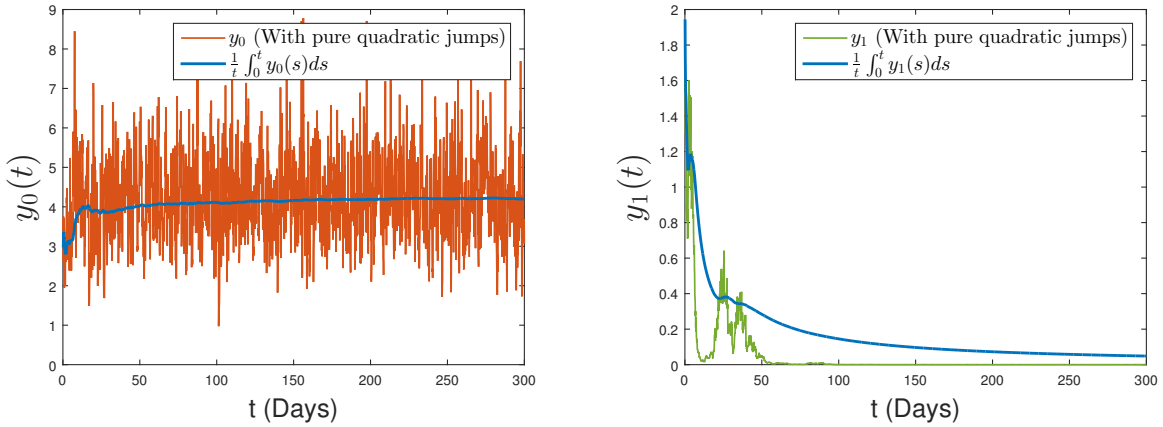

Figure 3. Conducting numerical simulations for solving system (4.1) in the presence of second-order jumps. In this case, we take $L = 2.5$ and $p = 0$. The jump intensities are defined as follows: $\nu_{00} = 0.01$, $\nu_{01} = 0.009$, $\nu_{10} = 0.02$ and $\nu_{11} = 0.007$. Here, we get $\theta_1 = 0.0526$ and $\theta_2 = 0.118$.

4.2. Case 2: Permanence and ergodicity of y_0 and y_1

We consider $L = 3.5$, $p = 0.5$ and we take the noise parameters as follows: $\varpi_{00} = 0.001$, $\varpi_{01} = 0.001$, $\varpi_{10} = 0.004$, $\varpi_{11} = 0.0012$, $\nu_{00} = 0.001$, $\nu_{01} = 0.001$, $\nu_{10} = 0.01$ and $\nu_{11} = 0.003$. In this case, we get $\theta_1 = 2.1982$ and $\theta_2 = 0.9862$. As per Theorem 3.2, there is a strong likelihood of the population y_0 and y_1 persisting, alongside the existence of a stationary distribution. This assertion is vividly illustrated in Figure 4.

We take $p = 1$ and we establish specific values for the white noise parameters $\varpi_{00} = 0.001$, $\varpi_{01} = 0.001$, $\varpi_{10} = 0.004$, $\varpi_{11} = 0.0012$. In this case, we get $\theta_1 = 2.1982$ and $\theta_2 = 1.3412$. Consequently, we have confirmed the fulfillment of the condition outlined in Corollary 3.3, ensuring the almost certain persistence of y_0 and y_1. This outcome is graphically illustrated in Figure 5, providing a visual representation of the verified result.

Now, we set $p = 0$. The jump intensities are defined as follows: $\nu_{00} = 0.001$, $\nu_{01} = 0.001$, $\nu_{10} = 0.01$ and $\nu_{11} = 0.003$. Here, we get $\theta_1 = 2.1982$ and $\theta_2 = 1.2981$. Henceforth, we have substantiated the fulfillment of the prerequisite delineated in Corollary 3.4. This validation is visually elucidated through the representation provided in Figure 6.

Expanding upon the insights drawn from the aforementioned figure, it becomes apparent that the characteristics of the noise exert a discernible influence on the magnitude of variation. Specifically, we observe a pronounced effect: as the intensity of the noise increases, there is a notable augmentation in the amplitude of variation. This correlation underscores the pivotal role played by noise levels in amplifying the variability within the system dynamics, thereby emphasizing the significance of noise intensity in shaping the observed outcomes.

Plankton size is a critical variable because it influences various biological and ecological processes. For example, smaller plankton may have faster reproduction rates but are more susceptible to predation, while larger plankton might be more resilient but have slower population growth. By studying different plankton sizes, we can observe how size-specific traits affect the overall population dynamics and stationary distribution. In instances of persistence, we explore the influence of plankton size and the

parameter p on the morphology of the stationary distribution, as illustrated in Figure 7. This detailed analysis illuminates the interplay between plankton size and system parameters, providing insights into how these factors shape the stationary distribution under varying conditions. By examining different plankton sizes and adjusting p , we can observe the impact on population dynamics and structure, ultimately gaining a deeper understanding of the conditions that favor particular plankton sizes and how populations adapt over time. This comprehensive examination is crucial for predicting plankton responses to environmental changes and for effective marine ecosystem management.

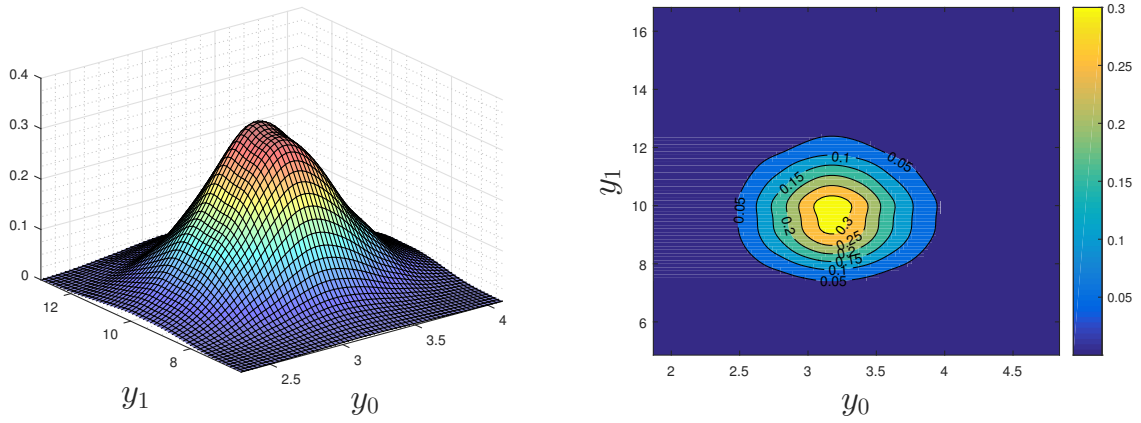

Figure 4. A three-dimensional visualization showcasing the stationary distribution, complemented by a two-dimensional contour plot illustrating the dynamics of system (4.1). In this case, $L = 3.5$ and $p = 0.5$. For noise intensities, we take $\varpi_{00} = 0.001$, $\varpi_{01} = 0.001$, $\varpi_{10} = 0.004$, $\varpi_{11} = 0.0012$, $\nu_{00} = 0.001$, $\nu_{01} = 0.001$, $\nu_{10} = 0.01$ and $\nu_{11} = 0.003$.

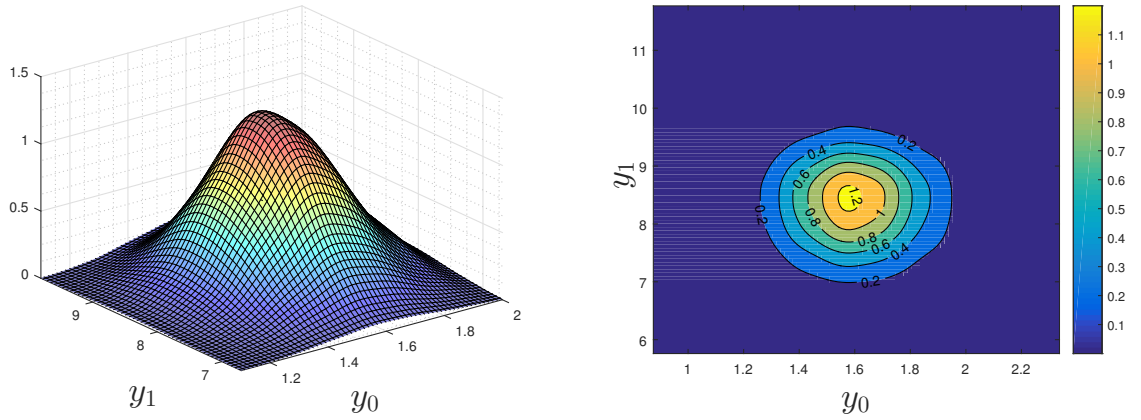

Figure 5. A three-dimensional visualization showcasing the stationary distribution, complemented by a two-dimensional contour plot illustrating the dynamics of system (4.1). In this case, $L = 3.5$ and $p = 1$. For noise intensities, we take $\varpi_{00} = 0.001$, $\varpi_{01} = 0.001$, $\varpi_{10} = 0.004$ and $\varpi_{11} = 0.0012$.

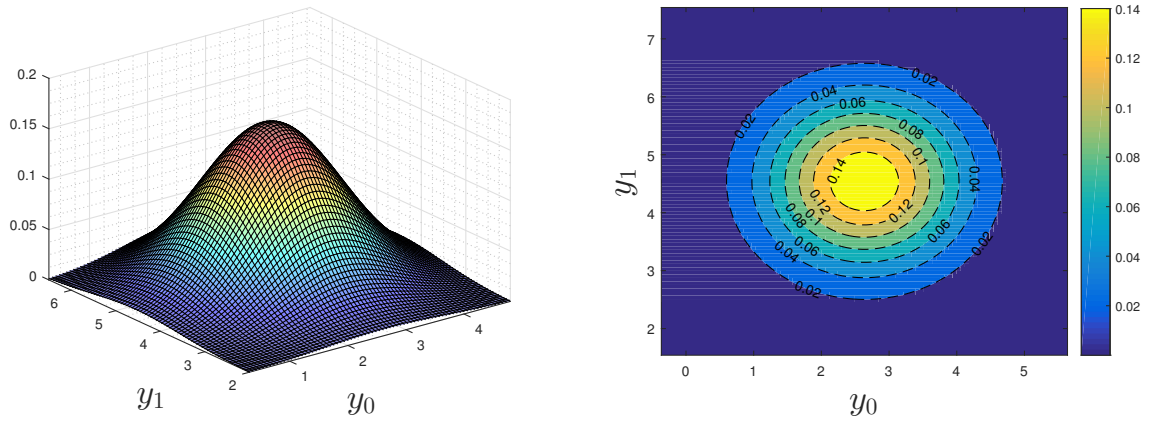

Figure 6. A three-dimensional visualization showcasing the stationary distribution, complemented by a two-dimensional contour plot illustrating the dynamics of system (4.1). In this case, $L = 3.5$ and $p = 0.5$. For noise intensities, we take $\nu_{00} = 0.001$, $\nu_{01} = 0.001$, $\nu_{10} = 0.01$ and $\nu_{11} = 0.003$.

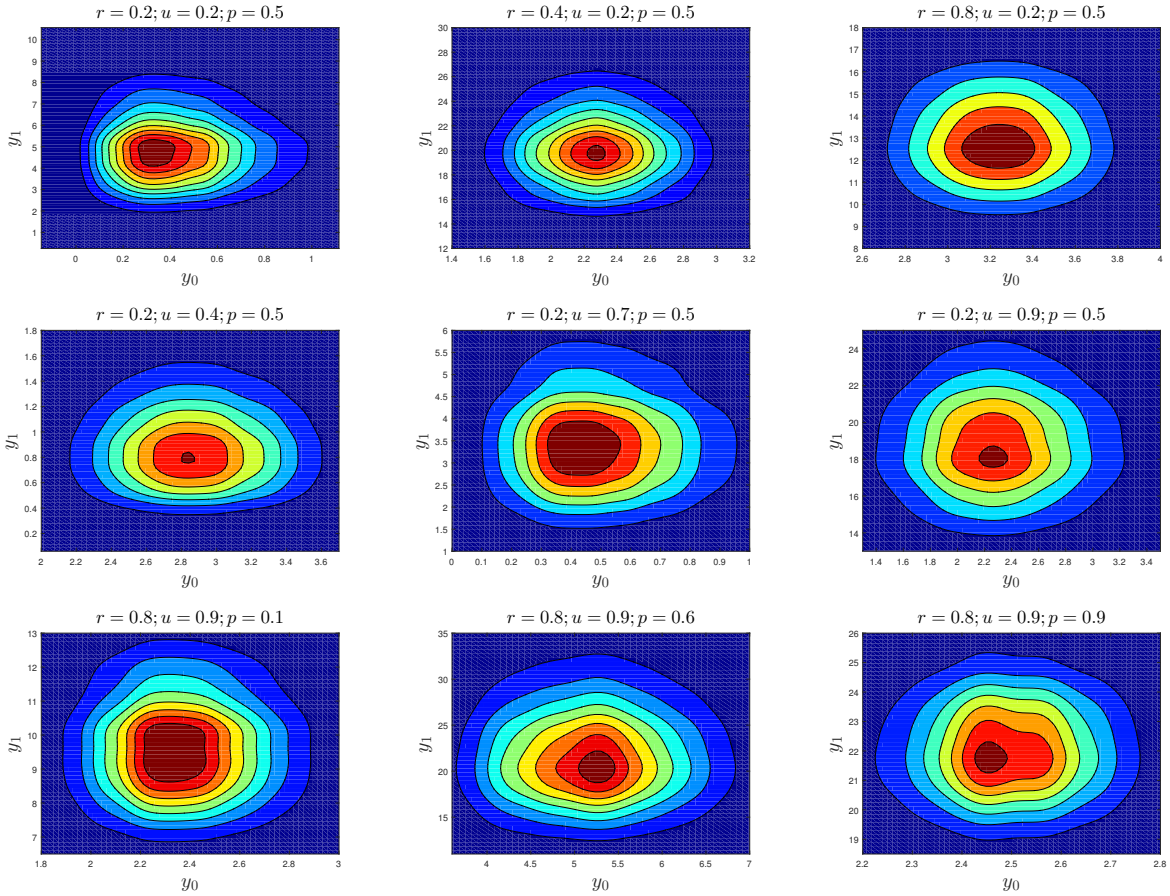

Figure 7. Numerical demonstration elucidating the profound impact of plankton size variations and parameter p fluctuations on the intricate morphology of the stationary distribution.

5. Conclusions

The stochastic dynamics inherent in marine ecosystems are of paramount importance, shaping the stability and resilience of these intricate environments. In this paper, we presented a novel nonlinear algae-zooplankton model, that offers a comprehensive framework for understanding the dynamics influenced by general interaction rates and second-order noise. Specifically, we distinguish between white noise and jump components, allowing for a detailed examination of their respective impacts on population dynamics.

Central to our investigation is the delineation of the global threshold that governs the delicate balance between species extinction and persistence. Through rigorous analysis, in Theorems 3.1 and 3.2, we probed the intricate interplay of various ecological factors, shedding light on the fundamental mechanisms underlying ecosystem dynamics.

In the numerical simulation section, we investigate the repercussions of noise on the long-term behavior of algae and zooplankton populations. By systematically varying parameters and plankton sizes, we unraveled the nuanced effects of noise intensity on population dynamics and stationary distributions. Through visual representations and quantitative analyses, we provided insights into how different types of noise shape the ecological trajectories of these crucial marine species, offering valuable implications for ecosystem management and conservation efforts.

The analysis described in this paper can be extended to describe the dynamics of a mycoloop model in aquatic food webs. This model involves interactions between phytoplankton, chytrids, and zooplankton [33]. By incorporating additional hypotheses and exploring more complex interactions, the model can provide deeper insights into the ecological processes governing mycoloop dynamics. We aim to pursue this idea in our future work, further enhancing our understanding of aquatic ecosystem dynamics.

Author contributions

Yassine Sabbar: Conceptualization, Writing Original Draft, Software, Formal Analysis; Aeshah A. Raezah: Conceptualization, Software, Validation. All authors have read and approved the final version of the manuscript for publication.

Use of AI tools declaration

The authors declare they have not used Artificial Intelligence (AI) tools in the creation of this article.

Acknowledgments

The authors extend their appreciation to the Deanship of Research and Graduate Studies at King Khalid University for funding this work through Large Research Project under grant number RGP 2/174/45.

Conflict of interest

The authors declare no conflict of interest.

References

1. S. Winkelmann, C. Schutte, *Stochastic dynamics in computational biology*, Springer, 2020.
2. N. S. Goel, N. R. Dyn, *Stochastic models in biology*, Elsevier, 2016.
3. D. J. Wilkinso, *Stochastic modelling for systems biology*, Chapman and Hall-CRC, 2006.
4. X. Mao, *Stochastic differential equations and applications*, Elsevier, 2007.
5. S. Zhang, T. Zhang, S. Yuan, Dynamics of a stochastic predator-prey model with habitat complexity and prey aggregation, *Ecol. Complex.*, **45** (2021), 100889. https://doi.org/10.1016/j.ecocom.2020.100889
6. Y. Zhang, B. Tian, X. Chen, J. Li, A stochastic diseased predator system with modified LG-Holling type II functional response, *Ecol. Complex.*, **45** (2021), 100881. https://doi.org/10.1016/j.ecocom.2020.100881
7. R. S. K. Barnes, R. N. Hughes, *An introduction to marine ecology*, UK: John Wiley and Sons, 1999.
8. R. V. Tait, F. Dipper, *Elements of marine ecology*, UK: Butterworth-Heinemann, 1998.
9. V. F. Krapivin, Mathematical model for global ecological investigations, *Ecol. Model.*, **67** (1993), 103–127. https://doi.org/10.1016/0304-3800(93)90001-9
10. V. Grimm, Mathematical models and understanding in ecology, *Ecol. Model.*, **75** (1994), 641–651. https://doi.org/10.1016/0304-3800(94)90056-6
11. T. Liao, Dynamical complexity driven by water temperature in a size-dependent phytoplankton zooplankton model with environmental variability, *Chinese J. Phys.*, **88** (2024), 557–583. https://doi.org/10.1016/j.cjph.2023.11.025
12. T. Liao, H. Yu, C. Dai, M. Zhao, Impact of cell size effect on nutrient-phytoplankton dynamics, *Complexity*, **2019** (2019), 1–23. https://doi.org/10.1155/2019/8205696
13. T. Liao, C. Dai, H. Yu, Z. Ma, Q. Wang, M. Zhao, Dynamical analysis of a stochastic toxin-producing phytoplankton-fish system with harvesting, *Adv. Differ. Equ.*, **2020** (2020), 1–22. https://doi.org/10.1186/s13662-020-02573-5
14. T. Liao, The impact of plankton body size on phytoplankton-zooplankton dynamics in the absence and presence of stochastic environmental fluctuation, *Chaos Soliton. Fract.*, **154** (2022), 111617. https://doi.org/10.1016/j.chaos.2021.111617
15. D. Kiouach, Y. Sabbar, Developing new techniques for obtaining the threshold of a stochastic SIR epidemic model with 3-dimensional Levy process, *J. Appl. Nonlinear Dyn.*, **11** (2022), 401–414.
16. D. Kiouach, Y. Sabbar, Dynamic characterization of a stochastic sir infectious disease model with dual perturbation, *Int. J. Biomath.*, **14** (2021), 2150016. https://doi.org/10.1142/S1793524521500169

17. Z. Yang, S. Yuan, Dynamical behavior of a stochastic nutrient-plankton food chain model with lévy jumps, *J. Nonlinear Model. Anal.*, **5** (2023), 415. https://doi.org/10.1007/s00216-022-04429-1

18. Y. Sabbar, A. Khan, A. Din, Probabilistic analysis of a marine ecological system with intense variability, *Mathematics*, **10** (2022), 2262. https://doi.org/10.3390/math10132262

19. J. E. Cohen, S. L. Pimm, P. Yodzis, J. Saldana, Body sizes of animal predators and animal prey in food webs, *J. Anim. Ecol.*, 1993, 67–78. https://doi.org/10.2307/5483

20. J. E. Cohen, T. Jonsson, S. R. Carpenter, Ecological community description using the food web, species abundance, and body size, *P. Natl. A. Sci.*, **100** (2003), 1781–1786. https://doi.org/10.1073/pnas.232715699

21. J. Memmott, N. D. Martinez, J. E. Cohen, Predators, parasitoids and pathogens: Species richness, trophic generality and body sizes in a natural food web, *J. Anim. Ecol.*, **69** (2000), 1–15. https://doi.org/10.1046/j.1365-2656.2000.00367.x

22. Q. Liu, D. Jiang, T. Hayat, A. Alsaedi, Dynamics of a stochastic predator-prey model with stage structure for predator and Holling type II functional response, *J. Nonlinear Sci.*, **28** (2018), 1151–1187. https://doi.org/10.1007/s00332-018-9444-3

23. Q. Liu, D. Jiang, Dynamical behavior of a higher order stochastically perturbed HIV-AIDS model with differential infectivity and amelioration, *Chaos Soliton. Fract.*, **141** (2020), 110333. https://doi.org/10.1016/j.chaos.2020.110333

24. D. Kiouach, Y. Sabbar, *Threshold analysis of the stochastic Hepatitis B epidemic model with successful vaccination and Levy jumps*, 2019 4th World Conference on Complex Systems (WCCS), IEEE, 2019. https://doi.org/10.1109/ICoCS.2019.8930709

25. Y. Sabbar, A. Din, D. Kiouach, Influence of fractal-fractional differentiation and independent quadratic Lévy jumps on the dynamics of a general epidemic model with vaccination strategy, *Chaos Soliton. Fract.*, **171** (2023), 113434. https://doi.org/10.1016/j.chaos.2023.113434

26. B. Zhou, B. Han, D. Jiang, Ergodic property, extinction and density function of a stochastic SIR epidemic model with nonlinear incidence and general stochastic perturbations, *Chaos Soliton. Fract.*, **152** (2021), 111338. https://doi.org/10.1016/j.chaos.2021.111338

27. Q. Liu, D. Jiang, Stationary distribution and extinction of a stochastic SIR model with nonlinear perturbation, *Appl. Math. Lett.*, **73** (2017), 8–15. https://doi.org/10.12968/nuwa.2017.Sup23.15

28. J. Rosinski, Tempering stable processes, *Stoch. Proc. Appl.*, **117** (2007), 677–707. https://doi.org/10.1016/j.spa.2006.10.003

29. D. Kiouach, Y. Sabbar, S. E. A. El-idrissi, New results on the asymptotic behavior of an SIS epidemiological model with quarantine strategy, stochastic transmission, and Levy disturbance, *Math. Method. Appl. Sci.*, **44** (2021), 13468–13492. https://doi.org/10.1002/mma.7638

30. N. Ikeda, S. Watanabe, A comparison theorem for solutions of stochastic differential equations and its applications, *Osaka J. Math.*, **14** (1977), 619–633.

31. Y. Sabbar, D. Kiouach, S. P. Rajasekar, S. E. A. El-idrissi, The influence of quadratic Levy noise on the dynamic of an SIC contagious illness model: New framework, critical comparison and an application to COVID-19 (SARS-CoV-2) case, *Chaos Soliton, Fract.*, **159** (2022), 112110. https://doi.org/10.1016/j.chaos.2022.112110

32. D. Zhao, S. Yuan, Sharp conditions for the existence of a stationary distribution in one classical stochastic chemostat, *Appl. Math. Comput.*, **339** (2018), 199–205. https://doi.org/10.1016/j.amc.2018.07.020

33. M. Chen, H. Gao, J. Zhang, Mycoloop: Modeling phytoplankton-chytrid-zooplankton interactions in aquatic food webs, *Math. Biosci.*, **368** (2024), 109134. https://doi.org/10.1016/j.mbs.2023.109134

AIMS Press